Earthquakes and Structures, *Vol. 7, No. 4 (2014) 571-586*
DOI: http://dx.doi.org/10.12989/eas.2014.7.4.571

Experimental and numerical investigations on seismic performance of a super tall steel tower

Minjuan He[1a], Zheng Li[*1], Renle Ma[1b] and Feng Liang[2c]

[1]*Department of Building Engineering, Tongji University, Shanghai, 200092, China*
[2]*Architectural Design & Research Institute of Tongji University (Group) Co., Ltd., Shanghai, 200092, China*

(Received July 7, 2014, Revised August 22, 2014, Accepted August 25, 2014)

Abstract. This paper presents experimental and numerical study on seismic performance of a super tall steel tower structure. The steel tower, with a height of 388 meters, employs a steel space truss with spiral steel columns to serve as its main lateral load resisting system. Moreover, this space truss was surrounded by the spiral steel columns to form a steel mega system in order to support a 12-story platform building which is located from the height of 230 meters to 263 meters. A 1/40 scaled model for this tower structure was made and tested on shake table under a series of one- and two-dimensional earthquake excitations with gradually increasing acceleration amplitudes. The test model performed elastically up to the seismic excitations representing the earthquakes with a return period of 475 years, and the test model also survived with limited damages under the seismic excitations representing the earthquakes with a return period 2475 years. A finite element model for the prototype structure was further developed and verified. It was noted that the model predictions on dynamic properties and displacement responses agreed reasonably well with test results. The maximum inter-story drift of the tower structure was obtained, and the stress in the steel members was investigated. Results indicated that larger displacement responses were observed for the section from the height of 50 meters to 100 meters in the tower structure. For structural design, applicable measures should be adopted to increase the stiffness and ductility for this section in order to avoid excessive deformations, and to improve the serviceability of the prototype structure.

Keywords: steel tower; seismic performance; shake table test; dynamic property; finite element model

1. Introduction

Quite a few television and broadcasting tower structures have been constructed around the world. The constructed towers are, typically, tall structures designed to support antennas for telecommunications, broadcasting, and television. These tower structures may also provide a platform for environment monitoring or sightseeing purposes. Super tall towers are normally slender structures. Earthquake- and wind-induced lateral deformation is one of the major structural concerns for such slender and flexible tall structures. Therefore, the lateral load resisting systems

∗Corresponding author, Ph.D. Candidate, E-mail: 09lizheng@tongji.edu.cn
[a]Professor, E-mail: hemj@tongji.edu.cn
[b]Professor, E-mail: marenle@tongji.edu.cn
[c]Senior Engineer, Ph.D., E-mail: lfcba@163.com

http://www.techno-press.org/?journal=eas&subpage=7 ISSN: 2092-7614 (Print), 2092-7622 (Online)

of super tall tower structures should be designed and constructed with enough stiffness in order to decrease the lateral deformation, and to ensure their safety and serviceability.

Research work has been reported on the theoretical analysis and experimental study for super tall TV and broadcasting towers. Riva *et al*. (1998) investigated the seismic performance of the Asinelli Tower in Bologna using finite element method. In order to evaluate the seismic performance of a 120m high concrete TV tower, Halabian *et al*. (2002) proposed a simplified pseudo-dynamic analysis procedure with the soil-structure interaction being taken into account. It was found that when the ductile behavior of the tower was considered in its structural design, the lateral response of the structure was very sensitive to the cracks in the reinforced concrete members. The seismic performance of the Tehran Telecommunication Tower was investigated numerically by Khaloo *et al*. (2001) and Yahyai *et al*. (2009). A finite element model considering the smeared cracks in reinforced concrete material for the tower structure was developed. In order to evaluate the dynamic characteristics of a tall steel TV Tower, an eigen-sensitivity based finite element (FE) model updating analysis was conducted by Wu and Li (2004). The model predictions (e.g. natural frequencies and vibration modes) were then verified by on-site measurement results. Vibration control and structural health monitoring for tall tower structures have also attracted much research attention. Techniques such as enlarging the damping ratio of the structure by incorporating energy dissipating dampers (Park *et al*. 2007; Walsh *et al*. 2012) and applying dynamic absorbers (Zhang *et al*. 2013) were investigated. For TV and broadcasting towers, Cao *et al*. (1998) presented the design of an active mass damper for a steel TV tower with a height of 310m. He and Ma (2001) investigated the effectiveness of the vibration control system for a steel TV tower with a height of 336m. On-site measurement was conducted, and the tuned mass damper which was placed in the tower at the height of 206m was proved to be very effective in decreasing its wind-induced vibration. Global Positioning System technology was used by Breuer *et al*. (2008) to monitor the deformation of the Stuttgart TV tower. The monitoring results were used to determine the displacement thresholds of the tower, and to examine the changes of its vibration characteristics. A complicated structural health monitoring system consisting of over 800 sensors has been implemented to Guangzhou TV Tower (Yi *et al*. 2012), which is a super tall steel tower structure with a height of 600m. Based on the monitoring data, a modal analysis was conducted by Chen *et al*. (2011), and the deformation of the tower under normal and typhoon conditions were calculated by Xia *et al*. (2014).

It should be noted that although the numerical analysis, vibration control and structural health monitoring for super tall TV and broadcasting tower structures have been extensively conducted, experimental researches on the seismic performance of such structures were quite limited. This study focuses on the seismic performance of a super tall steel TV and broadcasting tower structure. The prototype structure, Henan tower, with a height of 388 meters, is located in the city of Zhengzhou, China. The tower adopted a complex steel space truss with spiral steel mega columns as lateral load resisting system, and its platform building is located at the height of 230 meters. The tower is therefore classified as a vertically irregular structure. The construction site for Henan tower is one of the seismic prone zones in China. Thus, a thorough understanding of the overall dynamic behavior of Henan tower is crucial during its structural design. In this study, the seismic response of Henan tower was investigated both experimentally and numerically. A 1/40 scaled model for Henan tower was made and tested on shake table, and a nonlinear numerical model was developed. The dynamic characteristics and displacement response of the tower were obtained, and relative design recommendations were proposed.

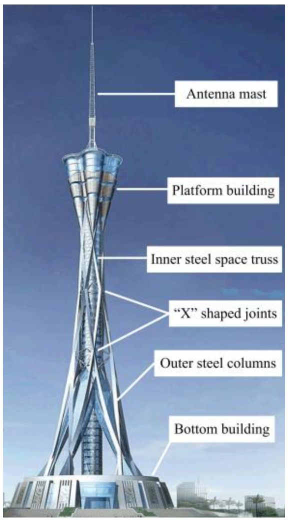

Fig. 1 Structural configuration of Henan tower

2. Description of the structure

Fig. 1 shows the structural configuration of Henan tower. It is composed of 5 parts (i.e., the bottom building, the inner steel space truss, the outer steel columns, the platform building, and the antenna mast). The bottom building of Henan tower is a six-story steel frame structure, and concrete shear walls were also placed around this steel frame structure to increase its lateral stiffness. The inner steel space truss system and the outer steel columns serve as the main lateral load resisting system. This inner steel space truss, which is a regular decagon space truss with a diameter of 14 meters, is surrounded by ten spiral outer steel columns with triangle cross sections. "X" shaped joints were designed at the intersections among these steel columns. In order to ensure the integrity of Henan tower, the outer steel columns and the inner space truss system are connected by steel braces at the height of 35 m, 70 m, 105 m, 148 m, 188 m, and 218.8 m, respectively. The platform building, which is a steel frame building and located at the height from 230 meters to 263 meters, serves as the observation deck for Henan tower, and it is composed of 12 stories with a total area of about 7000m^2. A quadrilateral space truss with a height of 125 meters was adopted for the antenna mast, which is located on the top of the tower.

3. Model Experiment

3.1 Model similitude and materials

In order to ensure that the test model behaves in a similar manner to the prototype, the model was designed by scaling down the geometric and material properties from the prototype structure in accordance with the dynamic similitude theory (Sabnis *et al*. 1983). Mild carbon steel Q235 with a yielding strength of 235 MPa was used for the steel members in the test model. Fine-aggregate concrete with fine wires was used for the reinforced concrete members in the test model.

Fig. 2 Overview of the test model on shake table

Table 1 Similitude scale factors for the test model

Parameter	Relationship	Model/Prototype
Length	S_1	1/40
Young's modulus	S_E	1.00
Stress	$S_\sigma = S_E$	0.68
Strain	S_σ / S_E	1.00
Density	$S_\sigma / S_\sigma S_1$	10.88
Force	$S_\sigma S_1^2$	4.25×10^{-4}
Frequency	$S_1^{-0.5} S_a^{-0.5}$	10.00
Acceleration	S_a	2.50

The dimension scaling parameter (S_l) was chosen as 1/40. The total height of the test model was 9.835 meters. The similitude scale factors for the modulus of elasticity (S_E) and stress (S_δ) were both equal to 1.0, and the similitude scale factor of acceleration (S_a) was set as 2.5. Additional mass blocks were evenly attached on the outer steel columns and the platform buildings in order to compensate for the difference in vertical load between the prototype and the test model. The total weight of the test model was 10.4 tons. Table 1 gives the similitude scale factors for the test model, and Fig. 2 demonstrates the overview of the model on shake table.

3.2 Shake table facility

Tests were carried out using the MTS shake table facility in Tongji University, China. Three-dimensional accelerations with six degree-of-freedoms can be applied to the test model at the same time by this shake table. The dimension of the shake table is 4m by 4m, and its maximum working load is 25 tons. The shake table can provide a maximum horizontal acceleration of 1.2g, and a maximum vertical acceleration of 0.7g. Its working frequency ranges from 0.1Hz to 50Hz, and there are 96 channels of data acquisition available during the testing process.

3.3 Data acquisition

The instrumentation was organized so that both overall and local responses of interest could be measured. Fig. 3 shows the data acquisition system and the installation of the test model.

26 accelerometers (i.e., AT1 ~ AT26) were installed on the inner core of the test model to monitor the structural accelerations. The bracketed numbers in Fig. 3(a) represent the actual height of measured point according to the prototype structure. There are two accelerometers installed at a specific height along the directions of X and Y, respectively. 8 linear voltage displacement transducers (i.e., DT1 ~ DT8) were installed on the test model to obtain its lateral displacements. It should be noted that the lateral displacements of the test model can also be obtained by integration of the structure's accelerations. Thus, the comparison between the displacement responses obtained by integration and that obtained by the LVDTs can serve as an indicator to evaluate the accuracy of the measurements. 18 strain gauges were placed on the "X" shaped joints in order to monitor the strain at the intersections among the outer steel columns.

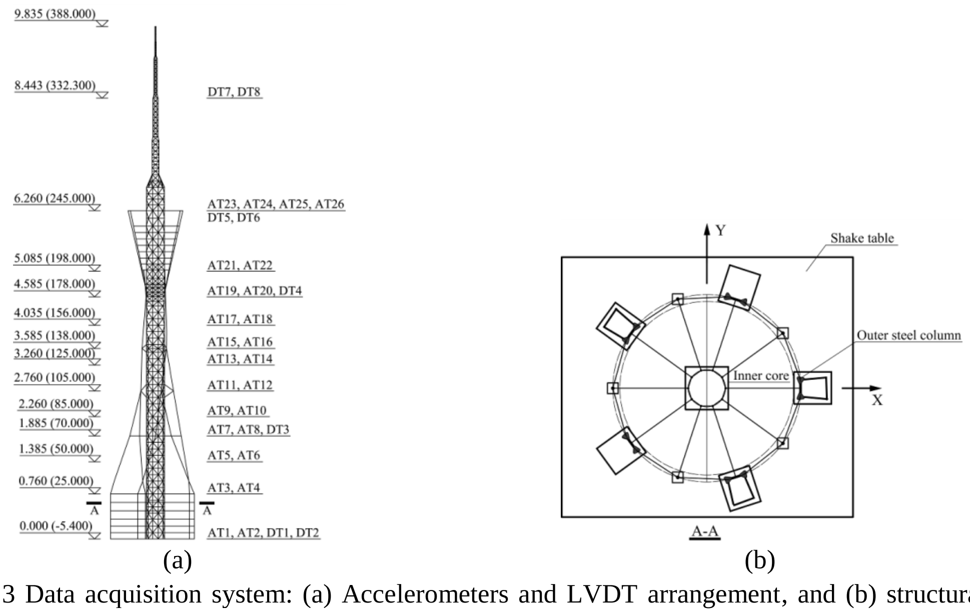

Fig. 3 Data acquisition system: (a) Accelerometers and LVDT arrangement, and (b) structural plan of the test model (all dimensions are in mm)

3.4 Test program

Henan tower is located in the city of Zhengzhou, which is classified as one of the seismic prone zones in China. Chinese Code for Seismic Design of Buildings (CCSDB, GB 50011-2011) has also defined minor, moderate and major earthquake hazard levels with the 50-year exceedance probabilities of 63%, 10% and 2% for the construction site of Henan tower, which are in accordance with the average return periods of 50, 475, and 2475 years, respectively. In this study, the peak ground accelerations (PGA) corresponding to minor, moderate and major earthquake levels are specified as 0.18g, 0.50g, 1.00g, respectively. Two historical earthquake ground motion records were selected as input excitations for the shake table test. In addition to these two records, the Zhengzhou artificial accelerogram (ZZW), which was provided by the Earthquake Administration of Zhengzhou, was also selected as an input excitation. The seismic inputs used in the shake table test are listed in Table 2.

Table 3 shows the detailed test program. For each earthquake record or accelerogram, two tests were performed with the main excitation firstly in the direction of X and then in the direction of Y. The tests were carried out in three phases representing minor, moderate, and major earthquake levels, respectively. After each series of ground acceleration inputs, white noise was applied to capture the natural frequencies and damping ratio of the test model.

Table 2 Seismic inputs

Number	Event	Time	Station
1	Imperial Valley	19/05/1940	El Centro Array #9
2	Kern county	21/07/1952	1095 Taft Lincoln School
3	Zhengzhou artificial	-	-

Table 3 Test program

Test phase	Test case	Signal	Principal direction	Input	Peak ground acceleration (g)		Note
					X direction	Y direction	
1st White noise	1	W1	The 1st white noise		0.05	0.05	Two-direction
Minor earthquake hazard level	2	F8EXY	X	El Centro	0.18	0.15	Two-direction
	3	F8EYX	Y		0.15	0.18	Two-direction
	4	F8TXY	X	Taft	0.18	0.15	Two-direction
	5	F8TYX	Y		0.15	0.18	Two-direction
	6	F8ZX	X	ZZW	0.18	-	Single-direction
	7	F8ZY	Y		-	0.18	Single-direction

Table 3 Continued

Test phase	Test case	Signal	Principal direction	Input	Peak ground acceleration (g)		Note
					X direction	Y direction	
2nd White noise	8	W2	The 2nd white noise		0.05	0.05	Two-direction
Moderate earthquake hazard level	9	B8EXY	X	El Centro	0.50	0.43	Two-direction
	10	B8EYX	Y		0.43	0.50	Two-direction
	11	B8TXY	X	Taft	0.50	0.43	Two-direction
	12	B8TYX	Y		0.43	0.50	Two-direction
	13	B8ZX	X	ZZW	0.50	-	Single-direction
	14	B8ZY	Y		-	0.50	Single-direction
3rd White noise	15	W3	The 3rd white noise		0.05	0.05	Two-direction
Major earthquake hazard level	16	S8EXY	X	El Centro	1.00	0.85	Two-direction
	17	S8EYX	Y		0.85	1.00	Two-direction
	18	S8TXY	X	Taft	1	0.85	Two-direction
	19	S8TYX	Y		0.85	1.00	Two-direction
	20	S8ZX	X	ZZW	1.00	-	Single-direction
	21	S8ZY	Y		-	1.00	Single-direction
4th White noise	22	W4	The 4th white noise		0.05	0.05	Two-direction

3.5 Results and discussions

3.5.1 Dynamic properties

The natural frequencies and damping ratios of the test model were obtained from the white noise phases. The frequencies and vibration modes of the test model and its corresponding prototype structure are listed in Table 4. The first three vibration modes of the test model are translation in direction X, translation in direction Y, and torsion, respectively. The first principle

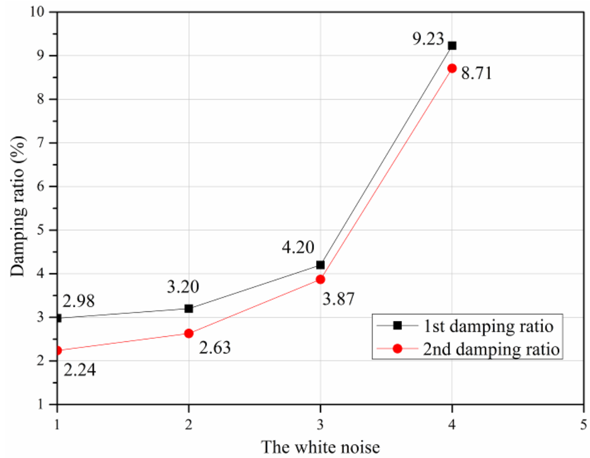

Fig. 4 Damping ratios of the test model

Table 4 Frequencies (Hz) of the test model and the prototype structure

Test phase	Category	Mode		
		1 Translation in X	2 Translation in Y	3 Torsion
Initial	Frequency_m[1] Frequency_p[2]	3.030 0.303	3.170 0.317	6.250 0.625
After excitations of minor earthquake level	Frequency_m Frequency_p	2.980 0.298	3.170 0.317	6.250 0.625
After excitations of moderate earthquake level	Frequency_m Frequency_p	2.930 0.293	3.130 0.313	6.250 0.625
After excitations of major earthquake level	Frequency_m Frequency_p	2.880 0.288	3.080 0.308	6.150 0.615

Note: [1] Frequency_m is the frequency of the test model;
[2] Frequency_p is the frequency of the prototype structure.

vibration mode is consistent with the test observation. It should be noted that the natural frequencies of the test model decreased gradually as the intensity of the seismic excitation increased, which implied a progressive degradation of structural stiffness. Fig. 4 shows the first two damping ratios of the test model which were obtained based on a power spectrum analysis. It is noted that the damping ratios of the test model increase slowly up to the moderate earthquake level. However, the damping ratios obtained from the 4th white noise phase were much larger than those obtained from the 3rd white noise phase, which indicated an obvious nonlinear behavior of the test model due to the developed damages under the major earthquake level.

3.5.2 Failure mode

For the test phase representing minor earthquake hazard level, no structural failure was observed in the test model. The displacement response at the main body of the test model was

(a)

(b)

Fig. 5 Failure modes: (a) Fracture in the antenna mast, and (b) local buckling of the outer steel column

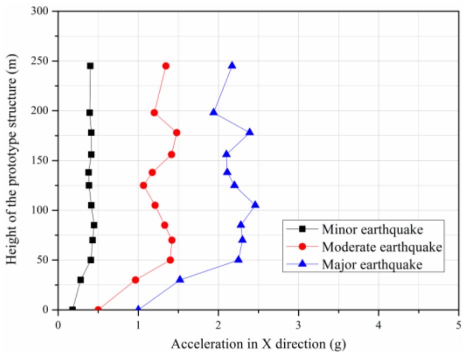

(a)

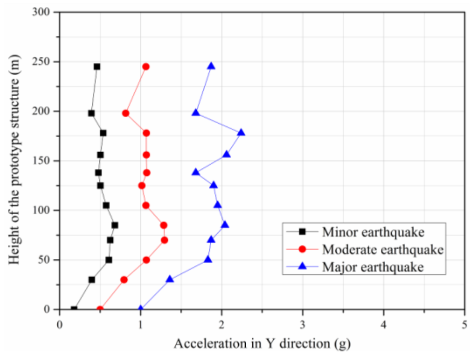

(b)

Fig. 6 Envelop curves of floor acceleration: (a) Acceleration in X direction, and (b) acceleration in Y direction

quite small. Results from the white noise test indicated that little change was developed in the model's frequency after the seismic excitations. The model behaved elastically, and no residual deformation was observed after this test phase. Similar results were obtained from the test phase of moderate earthquake level. No visual damage was observed in the steel members. However, some minor cracks were observed on the concrete shear walls in the bottom building of the test model.

Damages were observed in the test phase of major earthquake level after the Taft earthquake excitation (test case 18). As shown in Fig. 5(a), the antenna mast failed in the form of fracture at the height of 9.412 m, which was corresponding to 376.50 m for the prototype structure. This failure mode was mainly due to the cross sections of steel members in the antenna mast were quite small, and plumb weld was adopted to connect these small steel members. However, the strength of plumb weld was only about 40 N/mm^2, which was much lower than the strength of the weld used for steel members with regular size. Moreover, the lateral deformation of the antenna mast was quite large due to the whipping effect. Local bucking of the outer steel columns, as shown in Fig. 5(b), was also observed after this test case. The monitoring results from the strain gauges indicated that plastic regions were formed in a few steel members located between the height of 2.760 m and 4.585 m in the test model. However, the test model behaved in a ductile manner, and these local failures did not lead to the collapse of the test model.

3.5.3 Acceleration response

Fig. 6 shows the horizontal peak floor acceleration values of the test model obtained from the shake table test. It is noted that the maximum value of acceleration of 2.46g occurred in the direction of X under the excitation of major earthquake hazard level.

3.5.4 Displacement response of the prototype structure

For the test phase of minor earthquake of hazard level, the test model was featured in an elastic manner, and its inter-story displacement responses were quite small. However, as the earthquake input level being increased, damages in the form of fracture or local buckling occurred in the steel members. The stiffness of the test model decreased significantly, and its displacement response became much larger. The structural displacement of the prototype structure D_p can be calculated by Eq. 1.

$$D_P = \frac{a_{md} \times D_m}{a_{ma} \times S_d} \tag{1}$$

where D_m is the displacement response of the model in the shake table test, mm; a_{md} is the designed acceleration for the shake table test, g; and a_{ma} is the actual achieved acceleration by the shake table facility, g; S_d is the similitude scale factor of length, which is equal to 0.025.

Fig. 7 shows the envelop curves of the inter-story drift for the prototype structure under 250 meters, and the maximum inter-story drifts are also listed in Table 5. In the shake table test, the displacements of the antenna mast were not obtained since the difficulties in capturing the measurements. Moreover, for the antenna mast of a high-rising structure, larger inter-story drifts can always be allowed since the whipping effect. For the main body of steel tower structures, the

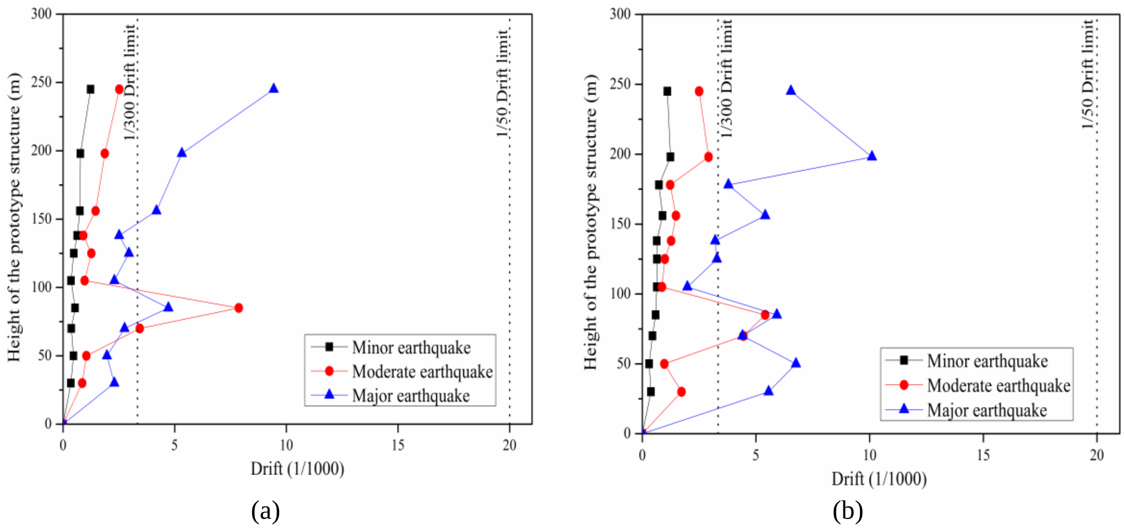

Fig. 7 Envelop curves of the inter-story drift for the prototype structure: (a) Inter-story drift in X direction, and (b) inter-story drift in Y direction

Table 5 Maximum inter-story drifts for the prototype structure

Test phase	X direction	Y direction
Minor earthquake level	1/810	1/807
Moderate earthquake level	1/127	1/185
Major earthquake level	1/106	1/99

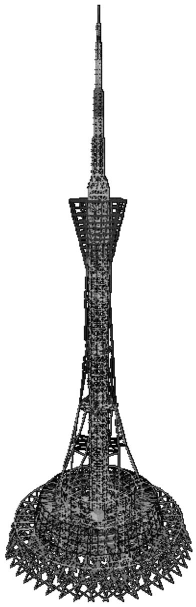

Fig. 8 Finite element model of Henan tower

Table 6 Frequencies (Hz) of the prototype structure (model prediction vs. test result)

Natural frequencies of Henan tower	Mode 1 Translation in X	Mode 2 Translation in Y	Mode 3 Torsion
Model prediction	0.234	0.236	0.493
Test	0.303	0.317	0.625

inter-story drift of 1/300 was normally adopted as the drift limit for minor earthquakes according to CCSDB, and the inter-story drift of 1/50 was normally adopted as the drift limit for major earthquakes. These drift limits are also shown in Fig. 7. It is noted that the inter-story driftsof the prototype structure are smaller than the respective drift limits. However, larger displacement response was observed for the section between the height of 50 meters and 100 meters. Forstructural design, applicable measures to increase the stiffness and ductility for this section, such as using stronger members, are recommended to be adopted in order to avoid excessive deformations, and to improve the serviceability of the prototype structure. The shake table test results in this study may also serve as verifications for numerical models, which can then be used to evaluate the seismic performance of the prototype structure under more realistic loading scenarios.

4. Numerical analysis

A nonlinear finite element model for Henan tower was developed using SAP2000 software. As shown in Fig 8, the steel members of the tower structure are modelled by 3-D Euler-Bernoulli beam elements, in which the shear deformation is ignored. In the finite element model, isotropic bilinear model, with a yielding strength of 345MPa, was used as material property for the steel members. For the minor and moderate seismic hazard level, the viscous damping ratio was set as 0.02. For the major seismic hazard level, the viscous damping ratio was set as 0.04 to consider the increase in the structure's damping. Moreover, the connections between the steel members in the finite element model were defined as pinned connected, which was in accordance with the structural design of the prototype structure.

4.1 Modal analysis

The natural frequencies of the tower structure obtained from the modal analysis are listed in Table 6. The first three vibration modes from the analysis were translation in direction X, translation in direction Y, and torsion, respectively, which were in accordance with the test results. However, the model predictions of the natural frequencies are about 25% lower than those obtained from dynamic test. This was mainly due the steel elements between the inner truss system and the outer steel columns were defined as pined connected in the finite element model. However, in the test model, welded connections, instead of the originally designed pinned connections, were adopted for those members. As a result, the test model behaved with a higher elastic stiffness under dynamic excitations. Moreover, a sensitivity study was also conducted to verify the influence of connection stiffness on the natural frequencies of the tower structure. It was noted that when the connections were modeled as fixed (welded) instead of pinned connected, the model predictions of the natural frequencies increased about 20%, which were closer with the test results.

4.2 Displacement and acceleration response

The earthquake records, as listed in Table 2, were also used as input for the nonlinear dynamic analysis. Similar to the test program, the analysis was conducted with the main excitation firstly in the direction of X and then in the direction of Y. For the minor and moderate seismic hazard level, since the steel members were still in the elastic range, the damage from the previous ground motions was not considered, and each seismic input was in accordance with a time history analysis using the same structural model without damage. However, for the major seismic hazard level, a single time history analysis was conducted with all ground motions stacked sequentially in order to consider the damage from the previous ground motions. Fig. 9 shows the envelop curves of the inter-story drift for the prototype structure obtained from the numerical analysis. Take the structural response in the direction of X for example, Fig. 10 shows the comparison of the results of inter-story drift obtained from the test and the numerical analysis, and Fig. 11 shows the comparison of the results of peak floor acceleration obtained from the test and the numerical analysis. It is observed that the model predictions of floor acceleration agreed relatively well with test results. It should be also noted that for minor earthquake level, the inter-story drift response obtained numerically was about 20% larger than that obtained experimentally. This was mainly due to the test model overestimated the lateral stiffness of the tower structure in the elastic stage.

However, for the major earthquake level, the inter-story drift response obtained numerically was only about 80% of that obtained experimentally. This was mainly due to the test model had already went through a few seismic excitations under minor and moderate earthquakes before the test phase of major earthquake level, and accumulated damages caused the degradation in the test model's stiffness. Larger displacement response was therefore observed from the test. It should also be noted from Fig. 10 that the deformation shape of the tower obtained from numerical analysis was quite similar to that observed from the shake table test. The predictions from the finite element model agreed reasonably well with the test results for both displacement response and deformation shape of the tower structure.

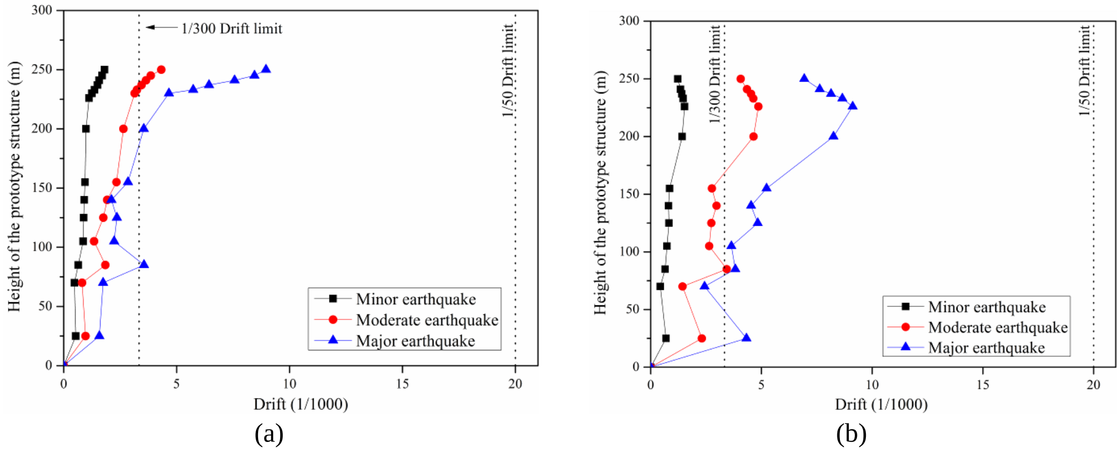

Fig. 9 Envelop curves of the inter-story drift obtained from numerical analysis: (a) Inter-story drift in X direction, and (b) inter-story drift in Y direction

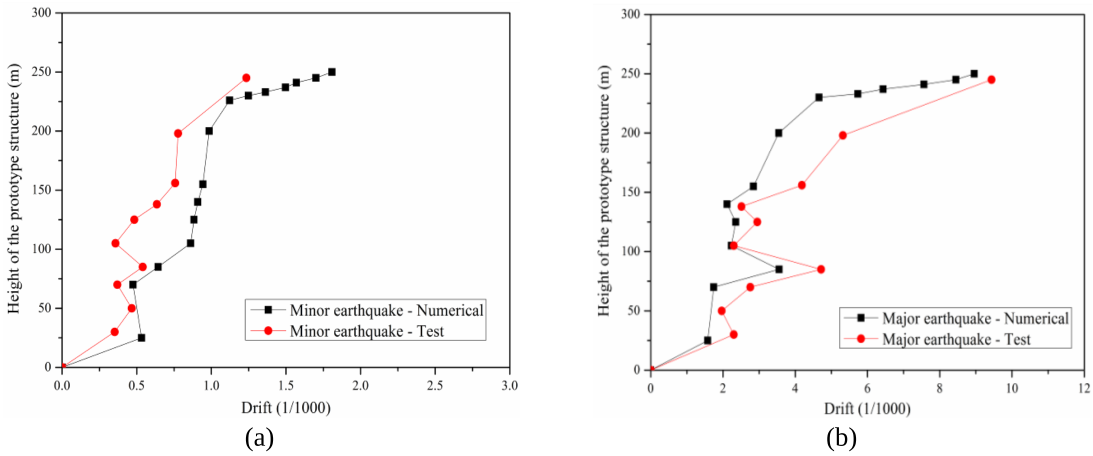

Fig. 10 Comparison of inter-story drifts from shake table test and numerical analysis in X direction: (a) Inter-story drift under minor earthquake, and (b) inter-story drift under major earthquake

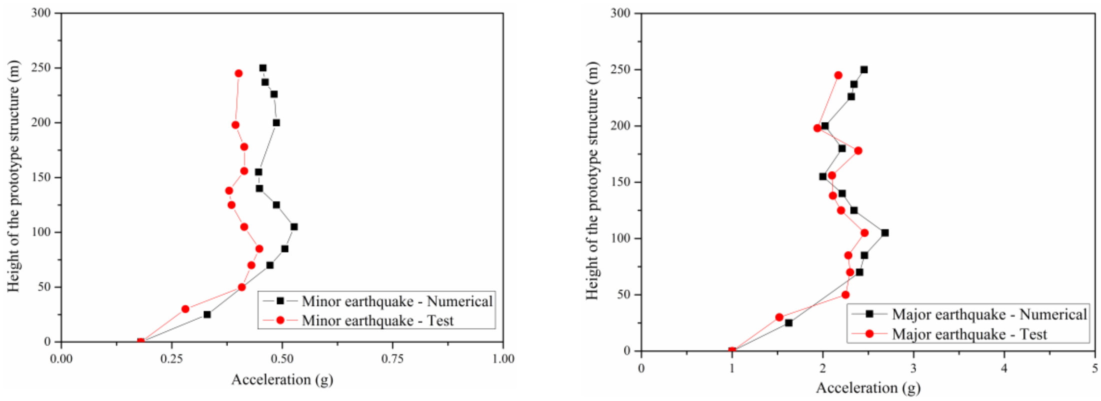

(a) (b)

Fig. 11 Comparison of acceleration from shake table test and numerical analysis in X direction: (a) Acceleration under minor earthquake, and (b) Acceleration under major earthquake

4.3 Stress status in steel

The stress status in the steel members under different levels of earthquakes was obtained from the numerical analysis. For the minor earthquake level considered in this study, the steel members were all in the elastic range. The von-mises stress for most of the steel members from the inner space truss was between 62MPa and 149MPa, while the von-mises stress for most of the steel members from the outer columns was between 78MPa and 157MPa. For the moderate earthquake level, although higher stress levels were observed, the steel members were still in the elastic range. The von-mises stress for most of the steel members from the inner space truss was between 104MPa and 279MPa, while the von-mises stress for most of the steel members from the outer columns was between 97MPa and 250MPa. For the major earthquake level, plastic regions were mainly observed in the steel columns located from the height between 50m to 100m, and some of them failed in the forming of yielding. In the shake table test, it was noted that some steel columns failed in the form of yielding along with local buckling. However, the plastic strain in most of members was shown to be much smaller than the ultimate plastic strain of steel, which indicated the tower behaved in a ductile manner without extensive or partial collapse.

5. Discussion

This paper investigates the seismic performance of a super tall steel tower. The dynamic properties, displacement responses, acceleration responses and failure modes of the tower structure were studied through shake table tests. It should be noted that the scaled model test provided meaningful information on the overall seismic performance of the prototype structure. What's more, the weak section of the prototype structure was also located through the analysis of the obtained displacement responses. More attention can therefore be paid to this weak section in the structural design process. However, the test was believed to overestimate the natural frequencies of the prototype structure, which was mainly due to that the simplified welded connections, instead of pinned connections, were adopted for the scaled model. A numerical model of the prototype structure was also developed. The model predictions were compared with the test results. It should be noted that the numerical model was based on full scale structure. However, in this study, the model predictions showed reasonable matches with the test results, and the numerical model was further used for the structure design of the prototype structure. For others cases, enough attention should be paid for the size effect during the validation of the numerical model.

6. Conclusions

The seismic performance of a super tall steel tower structure was investigated in this paper. A 1/40 scaled model of the prototype structure was subjected to a series of seismic ground motions. A finite element model for the prototype structure was then developed and verified by test results. It was noted that the model predictions of the dynamic characteristics and the displacement responses agreed reasonably well with test results. The test model performed elastically up to the moderate earthquake level, and it was able to withstand the major level of earthquakes with very limited damages. The displacement responses for the tower structure were also obtained. It is indicated by the drift responses that the weak section of the tower structure was located from the height of 50 meters to 100 meters. In structural design, attention should be paid to increase the stiffness and ductility of this section in order to avoid excessive deformations and to improve the serviceability of the prototype structure.

References

Breuer, P., Chmielewski, T., Gorski, P., Konopka, E. and Tarczynski, L. (2008), "The stuttgart TV tower - displacement of the top caused by the effects of sun and wind", *Eng. Struct.*, **30**(10), 2771-2781.

Cao, H., Reinhorn, A.M. and Soong, T.T. (1998), "Design of an active mass damper for a tall TV tower in Nanjing, China", *Eng. Struct.*, **20**(3), 134-143.

Chen, W., Lu, Z., Lin, W., Chen, S., Ni, Y., Xia, Y. and Liao, W. (2011), "Theoretical and experimental modal analysis of the Guangzhou New TV Tower", *Eng. Struct.*, **33**(12), 3628-3646.

Chinese Standard GB 50011-2011, Ministry of Housing and Urban-Rural Development of the People's republic of China (MOHURD). (2011), "Code for seismic design of buildings", Beijing, China (in Chinese).

Halabian, A.M., Naggar, M.H. and Vickery, B.J. (2002), "Nonlinear seismic response of reinforced-concrete free-standing towers with application to TV towers on flexible foundations", *Struct. Des. Tall Spec. Build.*, **11**(1), 51-72.

He, M.J. and Ma, R.L. (2001), "Measurements and analysis of the vibration of Heilongjiang broadcast and TV steel tower controlled by pendulous tank", *J. Build. Struct.*, **22**(1), 39-41, 57. (in Chinese)

Khaloo, A.R., Asadpour, N. and Horr, A.M. (2001), "Full dynamic analysis of Tehran telecommunication tower: linear and nonlinear responses", *Struct. Des. Tall Spec. Build.*, **10**(4), 263-281.

Park, J.H., Moon, B.W., Min, K.W., Lee, S.K. and Kim, C.K. (2007), "Cyclic loading test of friction-type reinforcing members upgrading wind-resistant performance of transmission towers", *Eng. Struct.*, **29**(11), 3185-3196.

Riva, P., Perotti, F., Guidoboni, E. and Boschi, E. (1998), "Seismic analysis of the Asinelli tower and earthquakes in Bologna", *Soil Dyn. Earthq. Eng.*, **17**(7-8), 525-550.

Sabnis, G.M., Harris, H.G. and White, R.N. (1983), "Structure modeling and experimental techniques", Englewood Cliffs, NJ.

Walsh, K., Cronin, K., Rambo-Roddenberry, M. and Grupenhof, K. (2012), "Dynamic analysis of seismically excited flexible truss tower with scissor - jack dampers", *Struct. Control Health Monit.*, **19**(8), 723-745.

Wu, J.R. and Li, Q.S. (2004), "Finite element model updating for a high-rise structure based on ambient vibration measurements", *Eng. Struct.*, **26**(7), 979-990.

Xia, Y., Zhang, P., Ni, Y.Q. and Zhu, H.P. (2014), "Deformation monitoring of a super-tall structure using real-time strain data." *Eng. Struct.*, **67**(5), 29-38.

Yahyai, M., Rezayibana, B. and Daryan, A.S. (2009), "Nonlinear seismic response of Milad tower using finite element model", *Struct. Des. Tall Spec. Build.*, **18**(8), 877-890.

Yi, T.H., Li, H.N. and Gu, M. (2012), "Sensor placement for structural health monitoring of canton tower", *Smart. Struct. Syst.*, **10**(4-5), 313-329.

Zhang, Z., Chen, J. and Li, J. (2013), "Theoretical study and experimental verification of vibration control of offshore wind turbines by a ball vibration absorber", *Struct. Infrastruct. Eng.*, **10**(8), 1087-1100.

IT